International Journal of Advanced Science and Research
www.allsciencejournal.com
ISSN: 2455-4227
Received: 10-10-2023, Accepted: 26-10-2023, Published: 11-11-2023
Volume 8, Issue 2, 2023, Page No. 1-6

Analysis of cellulose production from Cocos nucifera endocarps from a structural perspective

A F Afolabi
Department of Physics, Condensed Matter and Statistical Physics Research Unit, The Federal University of Technology, P.M.B., Akure, Nigeria

Abstract
Understanding the characteristics of organic materials is necessary for using them. This study set out to determine the characteristics of the separated cellulose from Cocos nucifera endocarps to determine its suitability for future use. To accomplish this, Cocos nucifera endocarp powder was alkaline pulped and chlorite bleached, and then the cellulose was subjected to various instrumental analyses using ImageJ software, Scanning Electron Microscopy (SEM), Fourier transform infrared (FTIR) spectroscopy and other tools. The existence of important cellulose functional groups such O-H, C-H, and C=O was confirmed by the FTIR. The cellulose appeared in the SEM micrograph as a cluster fiber with a rough surface that resembled a short rod. Using Visio 2016 and Origin PRO 2018, it was discovered that the average cellulose length and diameter are 56 mm and 20 mm, respectively, while the XRD revealed a mixture of crystalline and amorphous particles with 51% crystallinity and a crystallite size of 1.30 nm. The values of the total crystalline index and the lateral order index are 0.75 and 1.2, respectively. The findings might be used to assess the suitability of cellulose extracted from Cocos nucifera endocarps for various uses.

Keywords: *Cocos nucifera* endocarps, cellulose, crystallinity, pulping, bleaching, surface roughness

Introduction

Cocos nucifera endocarp is one of the biodegradable waste materials that does not decompose within a short period. This material can be converted to useful materials such as nanocellulose, cellulose plastics, hydrogel, membrane, and mechanical enhancers. Cellulose from agricultural waste is renewable and increasing rapidly in the progress of nanotechnology [1]. *Cocos nucifera* endocarp is mostly available in the vegetation zones in Nigeria (Okoroji *et al*., 2020). This material is very cheap, environmentally friendly and can be broken down by micro-organisms into simple organic molecules [2].

The biomass of *Cocos nucifera* endocarps consists of cellulose, lignin and hemicellulose. Cellulose is a flexible, composite and natural form of sugar found in plants or animals. Additionally, cellulose is a polymer with straight-chain crystalline units in groups as a result of intermolecular and intramolecular hydrogen bonding [3] and is visible as microfibrils under an electron microscope [4]. Cellulose molecules are arranged in crystalline regions and amorphous regions. Some methods such as synthetic and non-synthetic can be used to derive cellulose from various sources. Pure cellulose is normally extracted from plants using different pulping processes [3]. Chemical modification of cellulose is performed to produce cellulosic that can be adapted for different purposes. Cellulose is widely applicable in food products, composites, netting, upholstery, coatings, packing, paper, rope, clothing, electronics, construction, and so on [5]. Therefore, there is a need to produce low-cost cellulose from organic materials for several applications.

The research aims to isolate and analyse the structure of cellulose from Cocos nucifera endocarps.

Materials and Methods

1. Materials

Cocos nucifera endocarps were obtained from an area of global positioning system (GPS) coordinates of 7º 17′ latitude and 5º 9′ longitude with 355 meters altitude, Ondo State, Nigeria. The endocarp was removed from the back of the endosperm of a *Cocos nucifera* and used as a raw material for this research. The *Cocos nucifera* endocarp was dried and ground into particles using a Fritsch pulverizer. A 600 μm Sieve Shaker (Wiley Mechanical, England) was used to sieve the raw material and collect fine particles. Sodium hydroxide (NaOH), acetic acid (CH_3COOH) and sodium chlorite ($NaClO_2$) were purchased from Pascal Scientific Ltd and used as reagents.

2. Preparation of Cellulose

To obtain cellulose, 600 μm particles of *Cocos nucifera* endocarp (100 g) and NaOH (20%) before cooking (90$^{\circ}C$, 90 min) as earlier reported by Afolabi *et al.* (2021a). The material was washed free of alkaline after the reaction period and oven dry (105$^{\circ}C$). The obtained pulp material was bleached using sodium chlorite. Briefly, the pulp sample (10 g) was added to hot water (200 ml, 70$^{\circ}C$), then sodium chlorite (6 g) and CH_3COOH (1.5 mL). The mixture was allowed for half an hour in the water bath (70$^{\circ}C$). The addition of sodium chlorite (6 g), and CH_3COOH (1.5 mL) was repeated and the reaction continued (30 min). The bleached sample was obtained after filtration, washed free of chlorine and dry (105$^{\circ}C$).

Characterization of Cellulose

The isolated cellulose was analysed using X-ray diffraction (XRD), Scanning electron microscopy (SEM) and Fourier transform infrared (FTIR) spectroscopy techniques.

1. X-ray diffraction (XRD)

The crystal structure of the isolated cellulose from *Cocos nucifera* endocarps was evaluated by utilizing a Cu-Kα monochromator, Philips PW diffractometer at a voltage of 15kV, scanned along 2θ angle from 5° to 90°at wavelength λ=1.54Å.

Bragg's equation was utilized to acquire interplanar spacing (d-spacing) [6, 7]

$$d = \frac{n\lambda}{2sin\Theta} \quad (1)$$

where, Bragg's angle ($^{\circ}$) is θ, wavelength is λ(0.154nm) and interplanar spacing is d, order of reflection is n.

Segal *et al*. (1959) [8] method was used to calculate the crystallinity index ($C_r I$) estimated from the X-ray diffraction pattern [9]

$$C_{Ir} = \frac{I_{200} - I_{am}}{I_{200}} \times 100 \quad (2)$$

Where' intensity peak of the amorphous region at 2θ degrees is I_{am} and maximum intensity of the lattice diffraction is I_{200}.

Scherrer equation was used to obtain crystallite size (L) [10]

$$L = \frac{K \times \lambda}{B \times Sin\theta} \quad (3)$$

where, constant of value 0.91 is K, X-ray wavelength (0.1542 nm) is λ, intensity of the Full Width at Half Maximum (FWHM) is B and Bragg's angle (^{0}) is θ.

The proportion of crystallite interior chains or surface chains (X) [11]

$$X = \frac{(L - 2h)^2}{L^2} \quad (4)$$

where crystallite size is L and the layer thickness of the surface chain is $h = 0.57nm$.

The size distribution of the cellulose was determined using Microsoft Visio 2016, Origin Pro 8.5 software and the ratio:

$$\frac{unit\_value}{unit\_length} = \frac{length}{rel\_length} \quad (5)$$

The relative length (mm) was obtained from the Scanning Electron Micrograph using the line tool in Microsoft Visio 2016. 70 particles were considered whose both ends could be visibly seen.

Where unit value is the value of the magnification as obtained from the SEM micrograph given as 100 µm and the unit length is the length of the magnification bar measured using the line tool as 20.0882 mm. Thus:

$$Length\ (\mu m) = \frac{((relative\_length) * (1E-3) * (100E-6))}{20.0882E-3} \quad (6)$$

Similarly, the mean width of the nanoparticles was computed using the same method above

$$Width\ (\mu m) = \frac{((relative\_width) * (1E-3) * (100E-6))}{20.0882E-3} \quad (7)$$

2. Fourier Transform Infrared (FTIR)

Change in functional groups induced by several treatments within a wavelength range of 700–4000cm^{-1} was determined by Fourier transform infrared (FTIR) Spectrophotometer.

The infrared crystallinity (IR) ratio was evaluated using total crystalline index (TCI) [12, 13]

$$TCI = \frac{A_{1372}}{A_{2900}} \quad (8)$$

A_{1372} is the absorbance ratio from 1372 cm^{-1}, A_{2900} is the absorbance ratio 2900 cm^{-1}.

The lateral order index (LOI) was obtained from FTIR spectra [14] (Ciolacu *et al*., 2011)

$$LOI = \frac{A_{1427}}{A_{897}} \quad (9)$$

A_{1427} is the absorbance ratio 1430 cm^{-1} or 1420 cm^{-1}, A_{897} is the absorbance ratio 896 cm^{-1}

3. Morphological Characteristics

The morphology of the isolated cellulose was determined by the scanning electron microscopy (SEM) JEOL/EO JSM-6390 at 15 kV accelerated voltage and has a resolution of up to 100μm.

Results and Discussion

1. X-ray diffraction (XRD) Analysis

The diffractogram (Figure 1) of isolated cellulose from *Cocos nucifera* endocarps showed sharp peaks in Figure 1 with $15.82°, 21.89°$ and $34.49°$, which deduced crystalline phases of the cellulose. These three distinct crystalline peaks were characteristics of cellulose I which are similar to the X-ray diffraction patterns of cellulose extracted from rice husks [15] The peaks correspond to crystallographic planes (110), (200) and (004) which is in agreement with the result achieved by Abiaziem [1] from Sugarcane peels cellulose. The XRD micrograph presents the cellulose with both the amorphous and crystalline particles; the high intensity (21.89º) could be ascribed to the crystalline particle while the amorphous particle falls within the regions where there were no sharp peaks [16]. The high degree of crystallinity is a result of the crystal's growth in the crystalline regions and the broken bonds were well arranged during alkaline treatment [17, 18]. The calculated value of crystallite size is 1.30 nm and crystalline cellulose chains were densely packed with an interplanar spacing of 4.03 Å. The value of interplanar spacing is similar to the result obtained from delignification and bleaching for the production of Sago Frond cellulose [19]. The crystallinity index is 51%, the full width at half maximum is 0.11 and the surface chain is 0.06. All these parameters supported that the degree of crystallinity of the isolated cellulose is high, which is in agreement with the result obtained by Afolabi [20] from Moringa oleifera seeds cellulose.

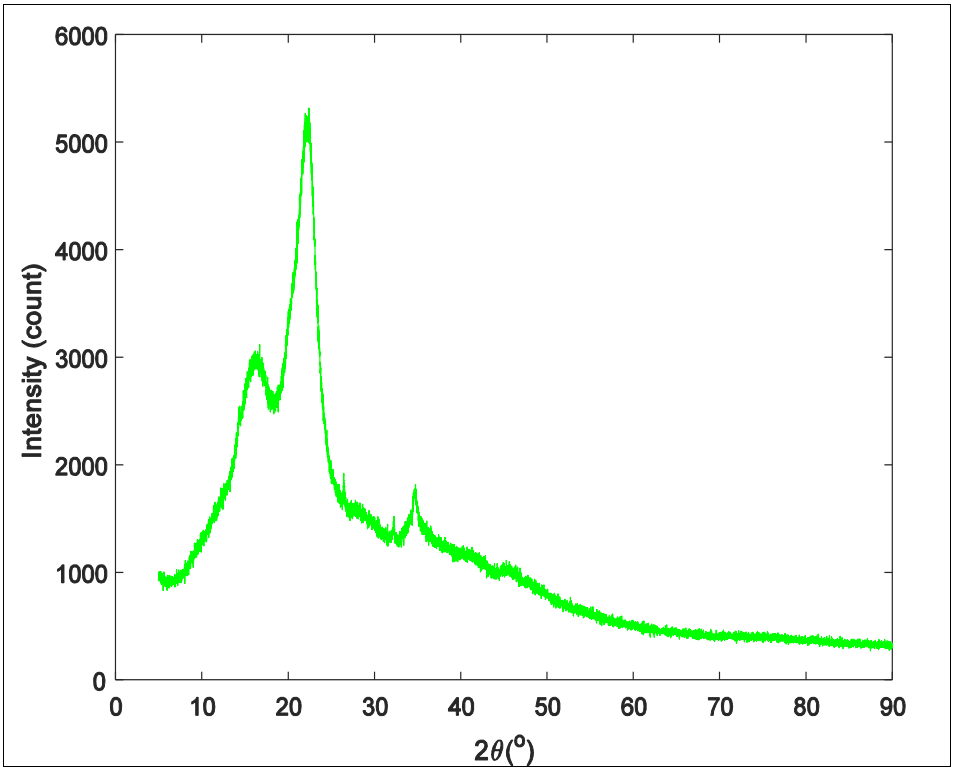

Fig 1: XRD of isolated cellulose from *Cocos nucifera* endocarps

2. Scanning Electron Microscopy (SEM) Analysis

The short-rod-like cluster fiber shape of the particles of the surface morphology of the isolated cellulose presented in Figure 2 is similar to the reported image for lignocellulosic corn agro-waste into cellulose and pharmaceutical application [21]. The particles are partially rough owing to the incomplete clear away of the lignin and hemicellulose [22]. It was noticed that the particles are agglomerated due to the high density of O-H groups on the molecule of cellulose chain surface in favour of the formation of hydrogen bonds [23]. Using Visio 2016 and Origin PRO 2018, it was revealed that the average length and diameter of the cellulose are 56μm and 20 μm respectively. This is in agreement with the results reported for structure, morphology and permeability of cellulose films [24].

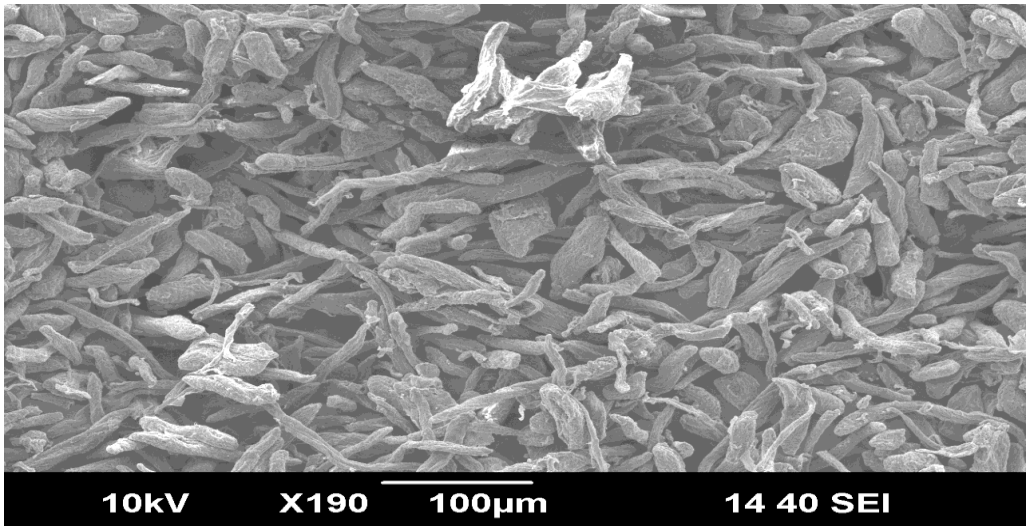

Fig 2: SEM of isolated cellulose from *Cocos nucifera* endocarps.

3. Surface Roughness

It was evident from the 3D image in Figure 3 that the isolated cellulose presents uneven surface morphology due to residual lignin after alkaline treatment. The surface roughness pattern of this study is similar to the result reported for three-dimensional microstructural properties of cellulose [25]. Surface roughness is significantly important to scientific applications owing to its indispensable position in chemical and physical interactions in various matters [26]. Additionally, the surface is also rough owing to the build-up and readjustment of the crystalline structure during the treatment [27]. The surface roughness is likely associated with the surface area with the large particle size [28]. This is similar to the result from previous research on the study of the particle size effects and properties, blending techniques and processing time on content uniformity [29].

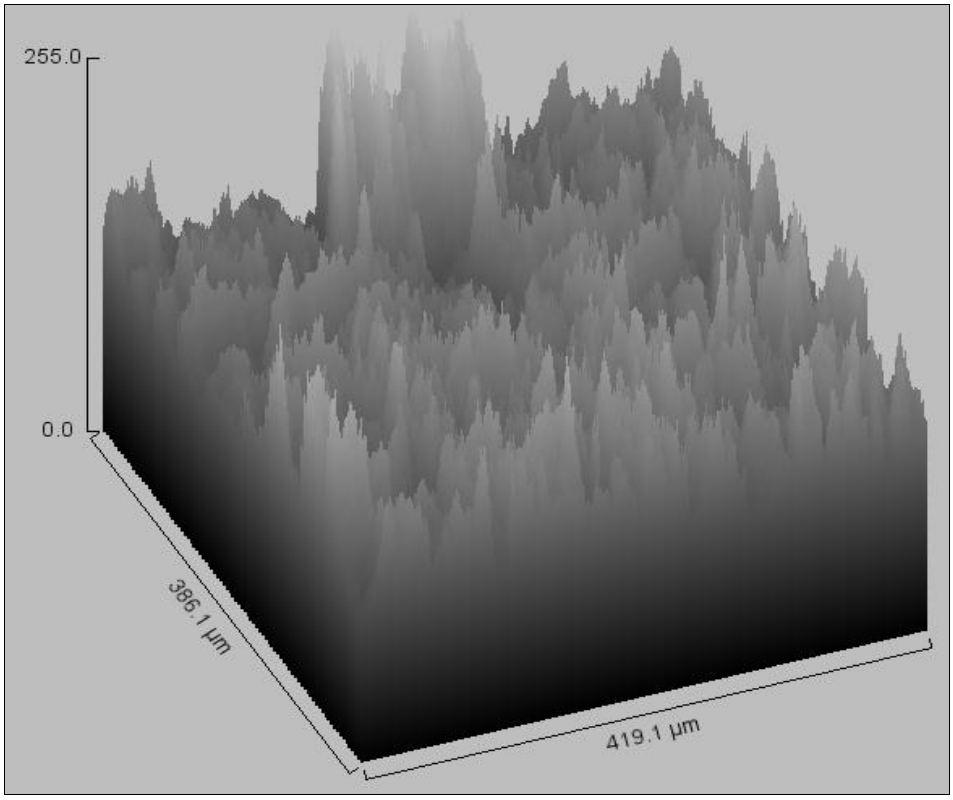

Fig 3: Surface roughness of isolated cellulose from *Cocos nucifera* endocarps.

4. Fourier Transform Infrared (FTIR) Analysis

The spectra of the Fourier transform infrared spectroscopy of the isolated cellulose in Figure 4 showed a wide band centered at 3332.5 cm^{-1} which specified O-H stretching vibration, whereas the stress at 2800-2950 cm^{-1} is ascribed to C-H of CH_2/CH_3 and a weak carbonyl group at 1750 cm^{-1} [30] These hydroxyl groups could be responsible for the crystalline structure of the cellulose [31] (Park *et al*., 2010). Various bands at 1300-1400 cm^{-1} showed the occurrence of -O- which joined with the carbon chain in the cellulose [32]. The peaks at 1021 cm^{-1} and 895 cm^{-1} were connected to the spectra characteristics of C-O stretching and C-H bending vibration of the isolated cellulose [33, 20].

The C-H bending vibration of the cellulose indicated the special formation as a result of β-glycosidic affinity with the glucose ring [34, 35]. The value of TCI is the same as the overall crystallinity degree of isolated cellulose which is 0.75 and the obtained result of LOI is 1.23 correlated to the whole amount of order in cellulose. These are in agreement with the finding of [36] on thermally modified properties of Oakwood and cellulose. The values of TCI and LOI were acquired from the FTIR spectra. These parameters revealed a high degree of crystallinity of cellulose. The values are in agreement with the findings of [37] on cellulose composites.

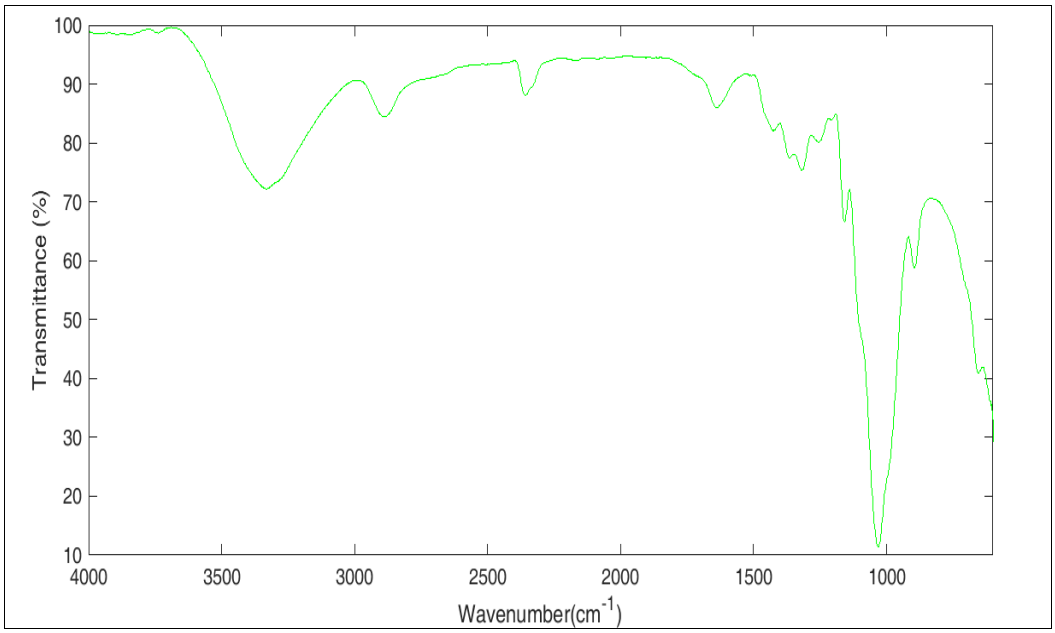

Fig 5: FTIR of isolated cellulose from *Cocos nucifera* endocarps

Conclusion

The structure of isolated cellulose from *Cocos nucifera* endocarps was investigated using alkaline treatment. Crystallographic planes from the X-ray diffraction are (110), (200) and (004). The XRD pattern revealed the crystalline structure with the most pronounced peak at 21.89°. Scanning electron micrograph showed that the particles are agglomerated. The average length and diameter of the cellulose are 56μm and 20μ m respectively. The surface roughness of the isolated cellulose from *Cocos nucifera* endocarps revealed the degree of irregularity of the surface. Furthermore, the surface is also rough owing to the growth and readjustment of the crystalline structure during the treatment. FTIR spectra showed the presence of hydroxyl groups (O-H) producing a well-arranged crystalline structure. In addition, the spectra characteristics of C-O stretching and C-H bending were revealed. It has a significant influence on the applications of cellulose in our environment.

Acknowledgements

The authors greatly appreciate Prof. G. Oboh for permission to carry out one part of the experiment of this research in the Phytomedicine Laboratory, Department of Biochemistry at the Federal University of Technology, Akure, Nigeria.

Funding

This research did not receive any specific grant from funding agencies in the public, commercial or not for profit sectors. It was self-funded work.

References

1. Abiaziem CV, Williams AB, Inegbenebor AI, Onwordi CT, Ehi- Eromosele CO, *et al*. Preparation and Characterisation of Cellulose Nanocrystal from Sugarcane Peels by XRD, SEM and CP/MAS ^{13}C NMR. IOP Conf. Series: Journal of Physics,2019:1299:012123. https://doi:10.1088/1742-6596/1299/1/012123.
2. Zaini LH, Jonobi M, Tahir PM, Karimi S. Isolation and characterization of cellulose whisker from kenaf (Hibiscus cannabinus) bast fibers. J. biomater. Nanobiotechnol,2013:4:37-44. https://doi:10.4236/jbnb.2013.41006.
3. Moeller M, Matyjaszewski K. Polymer Science: A Comprehensive Reference, first ed., Elsevier, Amsterdam, Netherlands, 2012.
4. Vietor RJ, Newman RH, Apperley DC, Jarvis MC. Conformational features of crystal-surface cellulose from higher plants. Plant J,2002:30:721-731.
5. Lavanya D, Kulkarni PK, Dixit M, Raavi PK, Krishna LNV. Sources of cellulose and their application A review. International Journal of Drug Formulation and Research,2011:2:19-38.
6. Kim UJ, Eom SH, Wada M. Thermal decomposition of native cellulose: influence on crystallite size. Polym. Degrad. Stab,2010:95:778-781. https://doi:10.1016/j.polymdegradstab.2010.02.009.
7. Adekoya MA, Oluyamo SS, Oluwasina OO, Popoola AI. Structural characterization and solid state properties of thermal insulating cellulose materials of different size classifications. Bioresour,2018:13:906-917. https://doi:10.15376/biores.13.1.906-917.
8. Segal L, Creely JJ, Martin AE, Conrad CM. An empirical method for estimating the degree of crystallinity of native cellulose using the X-ray diffractometer. Text. Res. J,1959:29:786-794. https://doi:10.1177%2F004051755902901003.
9. Gümüskaya E, Usta M, Kirei H. The effects of various pulping conditions on crystalline structure of cellulose in cotton linters. Polym. Degrad. Stab,2003:81:559–564. https://doi:10.1016%2FS0141-3910(03)00157-5.
10. Klug HP, Alexander LE. X-Ray diffraction procedures: for polycrystalline and amorphous materials, second ed., John Wiley & Sons, New York, 1956. https://doi:10.1016/0001-6160(56):90124-9.
11. Singh A, Ranawat B, Meena R. Extraction and characterization of cellulose from halophytes: next generation source of cellulose fibre. SN Applied Sciences,2019:1**:**1311. https://doi:10.1007/s42452-019-1160-6.
12. Khai DM, Nhan PH, Hoanh TD. An investigation of the structural characteristics of modified cellulose from acacia pulp. Vietnam J. Sci. Technol,2017:55:452-460. https://doi:10.15625/2525-2518/55/4/9216.
13. Singh JK, Sharma RK, Ghosh P, Kumar A, Khan ML. Imidazolium based ionic liquids: A promising green solvent for water hyacinth biomass deconstruction. Frontiers in Chemistry,2018:6:548-559. https://doi:10.3389/fchem.2018.00548.
14. Ciolacu D, Ciolacu F, Popa VI. Amorphous cellulose structure and characterization. Cellulose Chemistry and Technology,2011:45:13–21.
15. Ishak WHW, Amad I, Ramli S, Amin MCIM. Gamma irradiation-assisted synthesis of cellulose nanocrystal-reinforced gelatin hydrogels. Nanomaterials,2018:8:749. https://doi:10.3390/nano8100749
16. Sainorudin MH, Mohammad M, Kadir NHA, Abdullah NA, Yaakob Z. Characterization of Several Microcrystalline Cellulose (MCC)-Based Agricultural Wastes via X-Ray Diffraction Method. Solid State Phenomena,2018:280:340-345. https://doi:10.4028/www.scientific.net/SSP.280.340.
17. Kunusa WRI, Isa LA Laliyo, Iyabu H. FTIR, XRD and SEM Analysis of Microcrystalline Cellulose (MCC) Fibers from Corncorbs in Alkaline Treatment. IOP Conf. Series: Journal of Physics,2018:1028:012199. https://doi:10.1088/1742-6596/1028/1/012199.
18. Afolabi AF, Oluyamo SS, Fuwape IA. Synthetic characterization and structural properties of nanocellulose from moringa oleifera seeds. Journal of the Nigerian Society of Physical Sciences,2021b:3:148-153. https://doi: 10.46481/jnsps.2021.202.
19. Sunarti T, Arnata I, Suprihatin S, Farah F, Nur R. Cellulose Production from Sago Frond with Alkaline Delignification and Bleaching on Various Types of Bleach Agents. Oriental Journal Chemistry,2019:35:8-19. https://doi:10.13005/ojc/35Specialissue 102.
20. Afolabi AF, Oluyamo SS, Fuwape IA. Synthetic characterization of cellulose from moringa oleifera seeds and potential application in water purification. Journal of the Nigerian Society of Physical Sciences,2021a:3:140-143. https://doi:10.46481/jnsps.2021.206.
21. Rahman MS, Mondal MIH, Yeasmin MS, Sayeed MA, Hossain MA, Ahmed MB. Conversion of

Lignocellulosic Corn Agro-Waste into Cellulose Derivative and Its Potential Application as Pharmaceutical Excipient. Processes,2020:8:711. https://doi:10.3390/pr8060711.
22. Abdullah NA, Muhammad HS, Asim N, Mohammad M, Kadir NHA, Yaakob Z. Extraction of Microcrystalline Cellulose from Two Different Agriculture Waste via Chemical Treatment, 2020. IOP Conf. Series: Materials Science and Engineering 739 012017 https://doi:10.1088/1757-899X/739/1/012017.
23. Rehman N, Miranda MIG, Rosa SML, Pimentel DM, Nachtigall S, Bica CID. Cellulose and Nanocellulose from Maize Straw: An Insight on the Crystal Properties. Journal of Polymers and the environment,2014:22:252-259. https://doi: 10.1007/s10924-013-0624-9.
24. Makarov IS, Golova LK, Bondarenko GN, Anokhina TS, Dmitrieva ES, Levin IS, *et al*. Shambilova, Structure, Morphology and Permeability of Cellulose Films. Membranes,2022:12:297. https://doi: 10.3390/membranes12030297.
25. Miettinen A, Chinga-Carraso G, Kataja M. Three-Dimensional Microstructural Properties of Nanofibrilated Cellulose Films. International Journal of Molecular Sciences,2014:15:6423-6440. https://doi: 10.3390/ijms15046423.
26. Gong Y, Xu J, Buchanan RC. Surface roughness: A review of its measurement at micro-/nano-scale. Physical Sciences Reviews,2018:3:1-57. https://doi: 10.1515/psr-2017-0057.
27. Sainorudin MH, Mohammad M, Kadir NHA, Abdullah NA, Yaakob Z. Characterization of Several Microcrystalline Cellulose (MCC)-Based Agricultural Wastes via X-Ray Diffraction Method. Solid State Phenomena,2018:280:340-345. https://doi: 10.4028/www.scientific.net/SSP.280.340.
28. Sasahara Y, Kanatani K, Matsuhisa M, Wada Y, Shimizu R, Nishiyama N, *et al.* Impact of Surface Roughness on Recrystallization of an α-Al2O3(001) Single Crystal to α-AlO (OH) Diaspore Microcrystals. ACS Omega,2020:5:23520-23523. https://doi: 10.1021/acsomega.0c01376.
29. Alyami H, Dahmash E, Bowen J, Mohammed AR. An investigation into the effects of excipient particle size, blending techniques and processing parameters on the homogeneity and content uniformity of a blend containing low-dose model drug. PLOS ONE,2017:12:e0178772. https://doi: 10.1371/journal.pone.0178772.
30. Adel ZH, El-Wahabb AA, Ibrahim MT, Al-Shemy. Characterization of microcrystalline cellulose prepared from lignocellulosic materials. Part II: Physicochemical properties. Carbohydrate Polymers,2011:83:676-687. https://doi: 10.1016/jcarbpol.2010.08.039.
31. Park S, Baker JO, Himmel ME, Parilla PA, Johnson DK. Cellulose crystallinity index: measurement techniques and their impact on interpreting cellulase performance. Biotech- nol Biofuels,2010:3:10. https://doi:doi.org/10.1186/1754-6834-3-10.
32. Andalia R, Julinawati R, Helwati H. Isolation and characterization of cellulose from rice husk waste and sawdust with chemical method. Jurnal natural,2020:20:6-9. https://doi: 10.24815/jn.v20i1.12016.
33. Sultana T, Sultana S, Nur HP, Khan MW. Studies on mechanical, thermal and morphological properties of betel nut husk nanocellulose reinforced biodegradable polymer composites. Journal of Composites Science,2020:4:83-97.
34. Naduparambath S, Jinitha TV, Shaniba V, Sreejith Aparna MPKB, Purushothaman E. Isolation and characterisation of cellulose nanocrystals from sago seed shells. Carbohydrate polymers,2018:180:13–20 https://doi: 10.1016/j.carbpol.2017.09.088.
35. Singh JK, Sharma RK, Ghosh P, Kumar A, Khan ML. Imidazolium based ionic liquids: A promising green solvent for water hyacinth biomass deconstruction. Frontiers in Chemistry,2018:6:548-559. https://doi: 10.3389/fchem.2018.00548.
36. Hrcka R, Kucerova V, Hyrosova T, Honig V. Cell wall saturation limit and selected properties of thermally modified oak wood and cellulose. Forests,2020:2:640 https://doi: 10.3390/f11060640.
37. Poyraz B, Tozluogbu A, Candan Z, Demir A, Yavuz M, Buyuksari U, *et al*. Saka TEMPO-treated CNF Composites: Pulp and Matrix Effect. Fibres and Polymers,2018:19:195-204. https://doi: 10.1007/s12221-018-7673-y.